Evaluation Techniques for Motor Characteristics in JFE Steel

YOSHIZAKI Soichiro[*1]   ZAIZEN Yoshiaki[*2]   OKUBO Tomoyuki[*3]

Abstract:

JFE Steel established a technique to accurately measure motor characteristics under a wide range of motor drive conditions. Effect of core lamination and assembly methods on motor efficiency was experimentally evaluated by the technique. In 20JNEH1500, which is 3% Si steel with a sheet thickness of 0.2 mm, iron loss increased due to punching and shrink fitting, resulting in a significant decrease in efficiency in the low torque range. On the other hand, Si gradient steel 10JNHF600, which has Si distribution in the thickness direction, showed a smaller increase in iron loss than 20JNEH1500. From the above results, the application of Si gradient steel is suitable for shrink fitted motors and high efficiency small motors such as those used in drones.

1. Introduction

Because electrification is progressing in various fields, represented by the automotive sector, with the aim of realizing a carbon neutral society, motors are expected to be utilized in a wider range of applications than in the past. Since motors occupy about half of total world electric power consumption, improved motor efficiency will play an extremely important role in energy conservation[1]. Non-oriented electrical steel sheets are widely used as a core material for motors, and are a key component material that determins motor efficiency. In order to improve motor efficiency further reductions of the iron loss of electrical steels is strongly required, and various materials have been developed to meet this need[2–5].

JFE Steel fabricates and evaluates model motors using newly-developed electrical steel sheets, and has confirmed improvement in motor characteristics by evaluations based on actual measurement[6,7]. On the other hand, IPM (Interior Permanent Magnet) motors, which can be used under a wide range of operating conditions, have become the main stream in EV/HEV traction motors, and use of reluctance torque by vector control and downsizing achieved through higher motor rotating speeds are progressing[8]. However, because evaluations of the electric consumption of electric vehicles (EV) is not based on specified motor operating conditions, but on driving patterns such as WLTP (Worldwide harmonized Light duty driving Test Procedure), efficiency maps evaluation covering a wide motor operation region has now become necessary. Therefore, JFE Steel established a technique which enables accurate measurement of motor characteristics under a wide range of motor operating conditions. **Figure 1** shows an example of a motor efficiency map measurement result by this technique. The target of the evaluation was a model motor (8 poles, 48 slots) simulating an automotive traction motor, which was fabricated using the non-oriented electrical steel sheet 20JNEH1500 (thickness: 0.20 mm). Motor efficiency was measured under various conditions through stepwise changes in the current amplitude, phase angle and
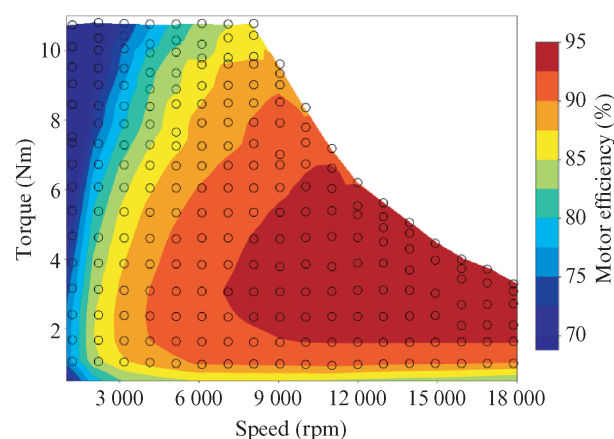

Fig. 1   Example of motor efficiency map evaluation

47

rotating speed, and the efficiency map was drawn for the current phase angle condition which achieved the maximum efficiency. The open circles (○) in the figure indicate the measurement evaluation points. This technique has made it possible to measure and evaluate the effects of the magnetic properties of electrical steel sheets and the core lamination and assembly method on motor characteristics under a wide range of drive conditions.

It is known that motor efficiency changes depending on the core lamination and assembly method[9,10]. **Figure 2** is a schematic diagram of the iron loss increase factors related to the motor core lamination and assembly process. It is known that iron loss is increased by processing distortion, which is introduced by the punching process, and by compressive stress due to shrink fitting. Since these are factors that prevent high efficiency in motors, a number of studies have been reported[11-13]. The present paper introduce examples of evaluation of the effect of lamination and assembly methods of electrical steel sheets on motor characteristics using the motor characteristics evaluation technique established in JFE Steel. Chapter 2 describes the results of an evaluation of the effect of shrink-fitting to fix the motor core for an IPM motor, and Chapter 3 discusses the results of an evaluation of the effects of punching and interlocking of the stacked core of a
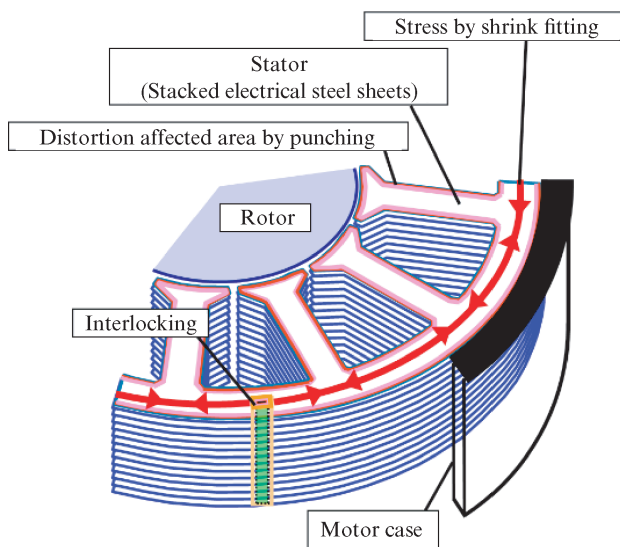
small SPM (Surface Permanent Magnet) motor with an outer rotor type, assuming use in drone applications.

2. Effect of Shrink Fitting on Motor Characteristics

This chapter presents the evaluation results of the effect of compressive stress on iron loss and the effect of shrink fitting on the motor characteristics for the non-oriented electrical steel sheet 20JNEH1500 and the Si gradient magnetic steel 10JNHF600. As shown in **Fig. 3**, the Si gradient steel JNHF™ has a Si concentration gradient in the thickness direction, in which the Si concentration in the surface layers is 6.5%, while the Si content in the central region is approximately 3%, and features low iron loss under high frequency conditions[14]. Since Si gradient steel is also known as a material that uniquely displays minimal changes in iron loss due to processing, it is expected to be effective for achieving higher efficiency in motors[15]. **Table 1** shows the representative magnetic properties of the two sample materials.

2.1 Experimental Method

First, the method of single sheet magnetic measurement under compressive stress will be explained. Single sheet samples with dimensions of 180 mm in length and 30 mm in width were prepared by shearing 20JNEH1500 and the Si gradient steel 10JNHF600. **Figure 4** shows the Single Sheet Tester (SST) used in the evaluation. Iron loss was measured under a condition in which compressive stress was applied in the magnetization direction of the single sheet sample. Buckling of the single sheet samples was prevented by applying planar pressure of 100 N by pressing a resin plate in the sample thickness direction.
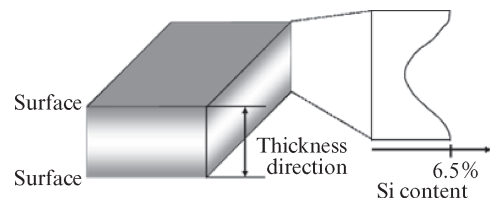
Next, the motor fabrication method will be

Fig. 2 Schematic diagram of iron loss increase factor

Fig. 3 Silicon distribution in Si gradient steel JNHF™

Table 1 Magnetic properties of Si gradient steel and conventional electrical steel

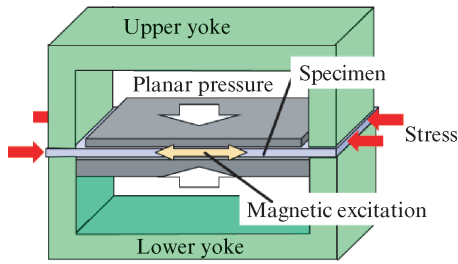| Material	Thickness (mm)	Magnetic flux density at 5 000 A/m, B_{50} (T)	Iron loss (W/kg)		
			$W_{10/400}$	$W_{10/1000}$	$W_{10/3000}$
Si gradient steel 10JNHF600	0.10 mm	1.53	10.1	30.0	100
3%Si steel 20JNEH1500	0.20 mm	1.66	12.5	47.3	231

Fig. 4　SST for magnetic measurement under stress

Table 2　Specification of test IPM motor

Items	Specification
Rated power output	3 kW
Input voltage	220 V_{de}
Current limit	20.0 Arms
Current phase angle	0.0-20.0 deg
Number of poles/slots	12/18
Outer diameter of stator	156.0 mm
Stacking length	25.0 mm
Winding connection	Three phase star connection, concentrated

explained. In order to evaluate the effect of shrink fitting on motor characteristics, cores fabricated using 20JNEH1500 and the Si gradient steel 10JNHF600 were assembled as motors under two conditions, i.e., with or without shrink fitting, and their motor characteristics were measured and evaluated. To extract and evaluate only the effect of shrink fitting, the cores were fabricated by a Wire Electrical Discharge Machining (Wire EDM) and gluing lamination process, which does not cause significant distortion. For the shrink fitting process, an aluminum alloy (AL5056) case was used with shrink fitting allowance of 0.045 mm. The compressive stress applied in the back yoke circumferential direction of the motor core was estimated to be approximately 50 MPa. Under the condition without shrink fitting, the core was glued with an adhesive on a motor case which was larger than the outer diameter of the motor core so that compressive stress was not applied to the core. **Table 2** shows the specification of the test motor. For motor control, the motor was driven by vector control using a PWM (Pulse Width Modulation) inverter, and motor characteristics were evaluated by mapping at the current phase angle which showed the highest efficiency at each measurement point.

2.2 Experimental Results and Discussion

First, the results of the single sheet magnetic measurements under compressive stress will be described. **Figure 5** shows the effect of compressive stress on the

iron loss of 20JNEH1500 and the Si gradient steel 10JNHF600. In 20JNEH1500, iron loss increased greatly depending on compressive stress, and an iron loss increase of around 50% could be seen under stress of 50 MPa or more. On the other hand, deterioration of iron loss due to compressive stress was slight in the Si gradient steel 10JNHF600 in comparison with 20JNEH1500, being no more than 5%. Since the Si gradient steel has internal stress, which originates from the difference in the Si concentration in the sheet thickness direction, it is thought the change in iron loss under compressive stress is small due to this feature[15].

Next, the motor evaluation results will be described. **Figure 6** shows results of the motor efficiency map evaluation. Although 20JNEH1500 showed a decrease in motor efficiency under the condition with shrink fitting in comparison with the condition without shrink fitting, almost no change in motor efficiency due to shrink fitting was seen in the Si gradient steel
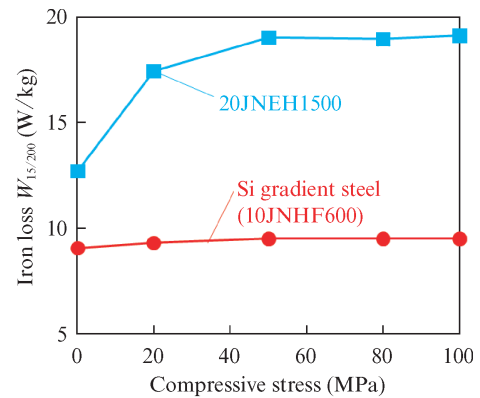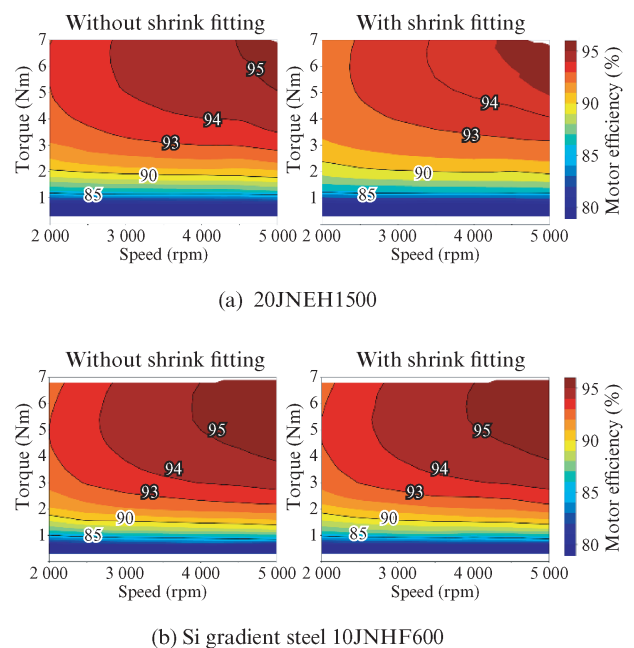

Fig. 5　Effect of compressive stress on iron loss

(a) 20JNEH1500

(b) Si gradient steel 10JNHF600

Fig. 6　Results of motor efficiency map evaluation

10JNHF600. **Fig. 7** shows the difference in motor efficiency due to the assembly conditions with and without shrink fitting. In the case of 20JNEH1500, motor efficiency decreased over a wide region, and a maximum decrease in motor efficiency of about 1 point could be seen in the low-load torque region. In the low-load torque region, the proportion of iron loss in total motor loss is large, suggesting that the effect of increased iron loss on motor efficiency is large. On the other hand, in the Si gradient steel 10JNHF600, the decrease in motor efficiency due to shrink fitting was clearly small in comparison with 20JNEH1500.

Figure 8 shows the result of separating motor loss into iron loss and copper loss when the motors were

driven at a rotating speed of 4 000 rpm and torque of 5.0 Nm in order to analyze the change in motor loss due to shrink fitting. Iron loss was separated by the following Eq. (1), and motor iron loss also includes mechanical loss and stray load losses such as leakage flux, *etc.*

$$P_{in} - P_{out} = P_{cu} + P_{Fe} \dots\dots\dots\dots\dots\dots\dots (1)$$

where, P_{in} is input power to a motor, P_{out} is motor output, P_{Cu} is copper loss and P_{Fe} is ion loss, and the values other than P_{Fe} were directly measured and evaluated. Copper loss did not change regardless of the core lamination and assembly method in both materials. However, the iron loss increase behavior due to shrink fitting differed depending on the material, and motor iron loss of 20JNEH1500 increased by approximately 14% as a result of shrink fitting, while almost no increase in iron loss due to shrink fitting was seen in the Si gradient steel 10JNHF600. It is thought that the Si gradient steel 10JNHF600 displays this behavior because the Si gradient steel is virtually unaffected by compressive stress, as was shown in Fig. 5. Thus, this study demonstrated that motors fabricated using Si gradient steel are not prone to the problems of decreased motor efficiency and increased iron loss accompanying shrink fitting.
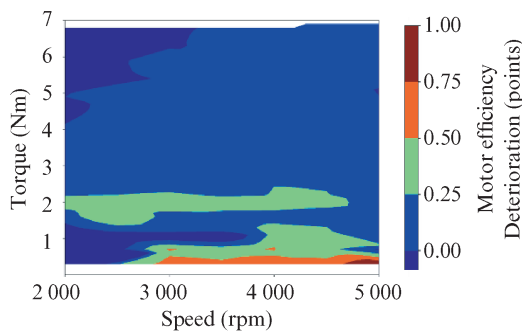
Based on the results described above, Si gradient steel is a suitable core material for motors in which shrink fitting is to be used because deterioration of iron loss due to compressive stress is slight, and high motor efficiency can be maintained even when motors are assembled by shrink fitting.

3. Effect of Punching on Motor Characteristics

This chapter present the study results on the effect of punching of electrical steel sheets on motor characteristics. A stress analysis utilizing synchrotron radiation and numerical analysis confirmed that residual stress occurs around the cut edge of electrical steel sheet as a result of punching[16,17]. The residual stress caused by punching has a large compressive component. This stress is a contributing factor to the increase in iron loss. Although depending on the material and the processing conditions, this type of deterioration of iron loss is thought to occur in the region around the punched edge, which means the adverse effect of punching easily appears in small motors with a narrow tooth width. Therefore, the change in motor characteristics due to punching of electrical steel sheets was evaluated in a small outer rotor-type SPM motor used in drone applications. The test materials were the same 20JNEH1500 and Si gradient steel 10JNHF600 as in
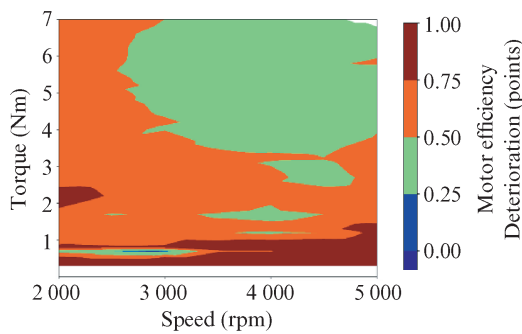
(a) 20JNEH1500

(b) Si gradient steel 10JNHF600

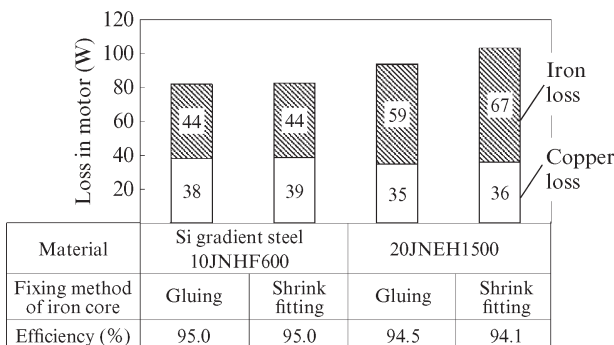Fig. 7   Comparison of motor efficiency maps

Material	Si gradient steel 10JNHF600		20JNEH1500	
Fixing method of iron core	Gluing	Shrink fitting	Gluing	Shrink fitting
Efficiency (%)	95.0	95.0	94.5	94.1

Fig. 8   Comparison of motor loss

Chapter 2.

3.1 Experimental Method

This section explains the iron loss evaluation method for materials simulating the effect of punching. As shown in the schematic diagram in **Fig. 9**, samples (rolling direction and perpendicular to rolling direction) with a length of 180 mm and widths of 5 mm, 7.5 mm, 10 mm, 15 mm or 30 mm were prepared by shearing. Although samples for use in magnetic measurements are normally machined with a width of 30 mm, the effect of residual stress introduced by punching or shearing becomes larger in samples with narrower widths. The narrow-width samples were first aligned in the widthwise direction and fixed with tape, and iron loss was then evaluated by the Epstein test.

Next, the motor evaluation method will be described. **Table 3** shows the specification of the SPM motor which was the object of evaluation. The object SPM motor is a small-scale motor with a tooth width of 1.5 mm, and is considered to be a type of motor in which the effect of punching on motor characteristics
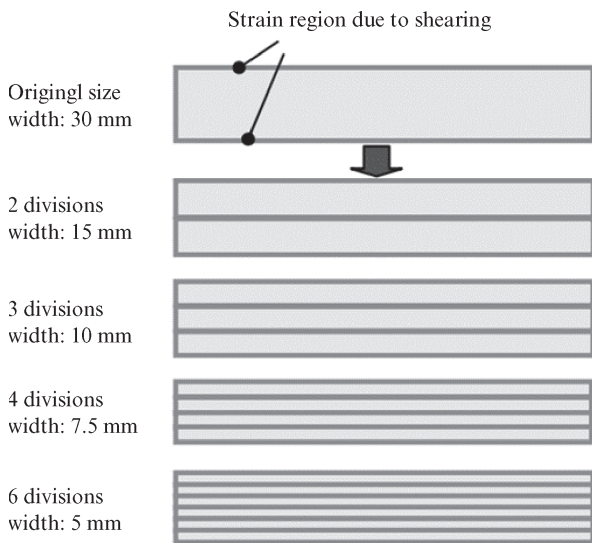
is particularly large. To evaluate the effect of the core lamination and assembly method on motor efficiency, cores were prepared by two methods, namely, "punching and interlocking" and "Wire EDM and gluing," and motor efficiency was evaluated. The samples were assembled by V-type interlocking with a depth of 0.35 mm, and interlocking dowels were arranged in all teeth. **Figure 10** shows a photograph of the appearance of the core fabricated using the Si gradient steel 10JNHF600. The motor efficiency of each of the fabricated motors was evaluated at various rotating speeds up to a maximum of 10 000 rpm.

3.2 Experimental Results and Discussion

First, the results of the iron loss evaluation by the Epstein test will be described. **Figure 11** shows the relationship between the sheared width of the magnetic measurement samples and iron loss. Since a tendency in which iron loss increased as the sample width became narrower was observed in all samples, it is thought that iron loss increased due to the effect of the residual stress introduced by shearing. In the 20JNEH1500, the iron loss of the 5 mm width sample was approximately 20% larger than that of the 30 mm width sample. On the other hand, it was found that increase in iron loss due to processing was substantially smaller in the Si gradient steel 10JNHF600, as the increase was limited to 5% or less. In Si gradient steel, which shows little increase in iron loss due to compres-
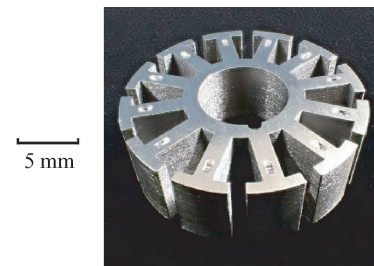

Fig. 9　Schematic view of sample

Table 3　Specifications of test SPM motor

Items	Specification
Rated power output	300 W
Input voltage	30 V_{de}
Current limit	20.0 Arms
Current phase angle	0.0 deg
Number of poles/slots	14/12
Outer diameter of stator	35.0 mm
Stacking length	10.2 mm
Winding connection	Three phase star connection, concentrated

Fig. 10　Appearance of motor core
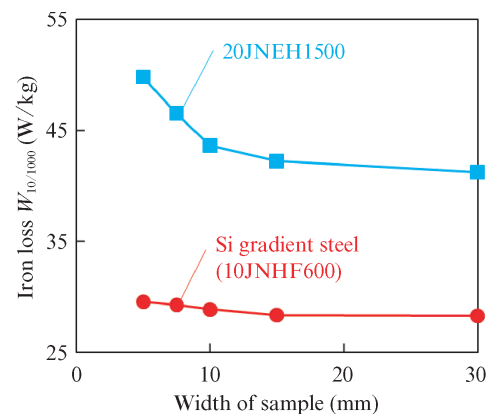
Fig. 11　Effect of sample width on iron loss

(a) 20JNEH1500

(b) Si gradient steel 10JNHF600

Fig. 12   Evaluation results of motor efficiency map
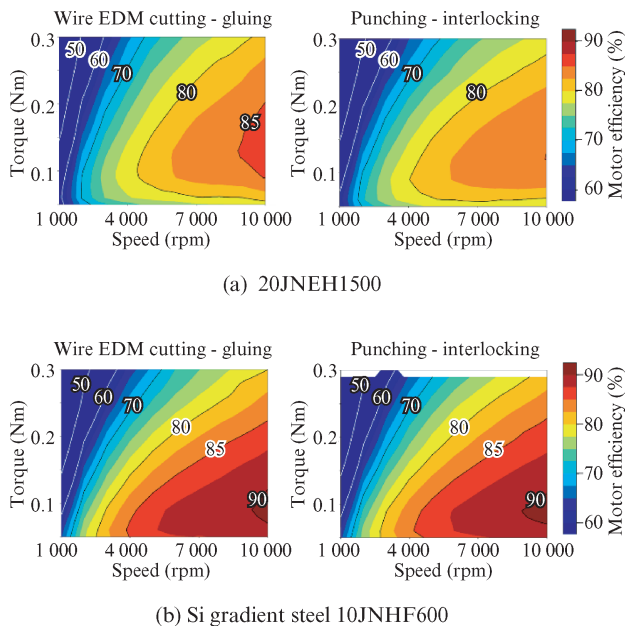

Fig. 13   Comparison of motor loss

sive stress, it is thought that effect of residual stress caused by shearing is slight, even if compressive stress occurs.

Next, the results of the motor evaluation will be described. **Figure 12** shows the motor efficiency maps for the Wire EDM method and the punching method. With 20JNEH1500, the map contained a region where operation with high efficiency exceeding 85% was possible when the Wire EDM method was used, but a similar high efficiency region was not observed with the punching method. In other words, a decrease in motor efficiency by punching was observed in the 20JNEH1500 material. On the other hand, with the Si gradient steel 10JNHF600, almost identical motor efficiency maps were obtained with both processing methods, and the change in motor efficiency due to the difference in the processing method was slight.

To compare the change in motor loss due to differences in core lamination and assembly methods, motor loss at the rotating speed of 10 000 rpm and torque of 0.1 Nm, which are near the maximum efficiency conditions, was separated into iron loss and copper loss. The results are shown in **Fig. 13**. Motor loss was separated by the same method as in section 2.2. In the case of 20JNEH1500, motor iron loss was larger with punching than with the Wire EDM method, but in contrast, the difference between iron loss with the Wire EDM method and the punching method was small with the Si gradient steel 10JNHF600.

From the results described above, it was found that the Si gradient steel shows little iron loss deterioration due to punching, and is an effective material for achieving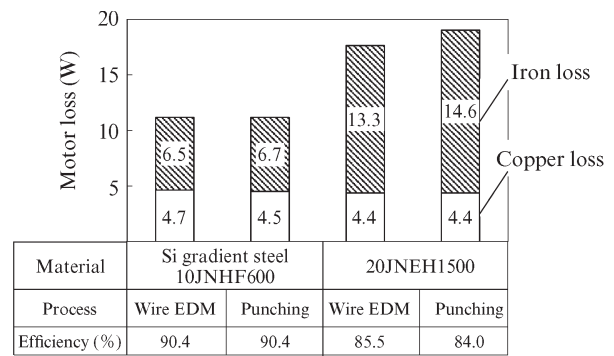 high efficiency in motors. In particular, because Si gradient steel has the feature of little deterioration of iron loss as a result of processing, it is considered to be a suitable core material for small motors, in which the effect of punching on iron loss easily appears.

4.   Conclusion

In this paper, the effects of core lamination and assembly methods for electrical steel sheets on motor efficiency were verified experimentally by using a motor evaluation technique that provides highly accurate results over a wide range of operating conditions. In addition, material evaluations simulating the effects of shrink fitting and compressive stress caused by punching on the iron loss of electrical steel sheets were carried out. As a result, in the case of the general electrical steel sheet 20JNEH1500, deterioration of iron loss by processing was observed in both the motor evaluation and the material evaluation. A wide-ranging evaluation of motor characteristics evaluation also demonstrated that the effect of the decrease in motor efficiency due to this deterioration of iron loss is large in the low-load torque region.

On the other hand, this study showed that the Si gradient steel 10JNHF600 displays deterioration of little iron loss due to punching, and thus can contribute to higher motor efficiency regardless of the core lamination and assembly method. In motors in which shrink fitting is performed to remove internal heat in a motor to the casing and small motors in which the core is manufactured by punching, it is difficult to achieve high efficiency due to the effects of processing of the steel sheets. Therefore, Si gradient steel, which is relatively unaffected by electrical steel sheet core lamination and assembly methods, is expected to be utilized in these types of motors.

[*]JNEH and JNHF are registered trademarks of JFE Steel Corporation.

References

1) Waide, P.; Brunner, C. Energy-Efficiency Policy Opportunities for Electric Motor-Driven Systems. IEA Energy Papers. 2011, 128 p.

2) Toda, H.; Senda, K.; Ishida, M. Effect of Material Properties on Motor Iron Loss in PM Brushless DC Motor. IEEE Trans. Magn. 2005, vol. 41, p. 3937–3939.

3) Yoshizawa, K. Development Trend and Outlook for Soft Magnetic Materials. Materia Japan. 2017, vol. 56, no. 3 p. 186–189.

4) Hayakawa, Y. Recent Developments in Non-Oriented Electrical Steels. Tetsu-to-Hagane. 2020, vol. 106, no. 10, p. 683–696.

5) Electrical Steels for EV Traction Motors in JFE Steel. JFE Technical Report. 2022, no. 27, p. 95–98.

6) Toda, H.; Oda, Y.; Kohno, M.; Ishida, M.; Zaizen, Y. A New High Flux Density Non-Oriented Electrical Steel Sheet and its Motor Performance. IEEE Trans. on Magnetics. 2012, vol. 48, no. 11, p. 3060–3063.

7) Toda, H.; Senda, K.; Morimoto, S,; Hiratani, T. Influence of Various Non-Oriented Electrical Steels on Motor Efficiency and Iron Loss in Switched Reluctance Motor. IEEE Trans. on Magnetics. 2013, vol. 49, no. 7, p. 3850–3853.

8) Mizutani, R. Technical Transition of Motors for Hybrid Vehicles. IEEJ Journal. 2018, vol. 138, no. 5, p. 288–291.

9) Yoshizaki, S.; Zaizen, Y.; Okubo, T.; Oda, Y. Effect of Punching on Efficiency of Drone Motor. Proceedings of the IEE Japan Industry Applications Society Conference 2022, ronbun no. 3–66, p. 314–315.

10) Yoshizaki, S.; Senda, K.; Zaizen, Y.; Oda, Y. Evaluation of shrink-fitting IPM motor using Si gradient steel in wide range operation. Annual Meeting Record, I.E.E. Japan. 2021, ronbun no. 5–041, p. 74–75.

11) Doi, S; Aoki, T.; Okazaki, K.; Takahashi, Y.; Fujiwara, K. Study of Computation Method of Iron Loss Considering Magnetic Isotropic by Processing Residual Stress. IEEJ Transactions on Power and Energy. 2018, vol. 138, no. 1, p. 36–44.

12) Yamaguchi, S.; Daikoku, A.; Tani, Y.; Tanaka, T.; Fujino, C. Accurate Magnetic Field Analysis for Estimating Motor Characteristics Considering Deteriorated Magnetic Properties in Magnetic Core Due to Stamping. IEEJ Journal of Industry Applications. 2015, vol. 135, no. 1, p. 1107–1115.

13) Toda, H.; Zaizen, Y.; Namikawa, M.; Shiga, N.; Oda, Y.; Morimoto, S. Iron loss deterioration by shearing process in non-oriented electrical steel with different thicknesses and its influence on estimation of motor iron loss. IEEJ Journal of Industry Applications. 2014, vol. 3, no. 1, p. 55–61.

14) Namikawa, I.; Ninomiya, H.; Yamaji, T. High Silicon Steel Sheet Realizing Excellent High Frequency Reactor Performance. JFE Technical Report. 2005, no. 8, p. 11–16.

15) Oda, Y.; Hiratani, T.; Kasai, S.; Okubo, T.; Senda, K.; Chiba, A. Effect of Compressive Stress on Iron Loss of Gradient Si Steel Sheet. IEEJ Journal of Industry Applications. 2015, vol. 135, no. 12, p. 1199–1206.

16) Fukumura, M.; Zaizen, Y.; Omura, T.; Senda, K.; Oda, Y. Visualization of Hydrogen in Stress and Strain Fields Using SIMS. ISIJ International. 2018, vol. 59, no. 688, p. 65–70.

17) Zaizen, Y.; Omura, T.; Fukumura, M.; Senda, K.; Toda, H. Evaluation of stress distribution due to shearing in non-oriented electrical steel by using synchrotron radiation. AIP Advances6. 2016, 055926